EAST EUROPEAN JOURNAL OF PHYSICS. 1. 141-150 (2025)
DOI:10.26565/2312-4334-2025-1-13 ISSN 2312-4334

PERFORMANCE ENHANCEMENT OF InGaP/GaAs DUAL-JUNCTION SOLAR CELLS THROUGH BSF LAYER OPTIMIZATION AND HETERO-TUNNEL JUNCTION

Ikram Zidani[a]*, Zouaoui Bensaad[a], Loumafak Hafaifa[b,c], Hamza Abid[a], Ahmed Hafaifa[d]
[a]*Applied Materials Laboratory, Djilali Liabes University, Sidi Bel Abbes, Algeria*
[b]*Department of Physics, Faculty of Exact Sciences and Computer Science, Ziane Achour University, 17000 Djelfa, Algeria*
[c]*Physico-Chemistry of Materials and Environment Laboratory, Ziane Achour University, BP 3117, Djelfa, Algeria*
[d]*Applied Automation and Industrial Diagnostics Laboratory, Faculty of Science and Technology, University of Djelfa 17000 DZ, Algeria*
**Corresponding Author e-mail: ikram.zidani@univ-sba.dz*
Received October 9, 2024; revised December 18, 2024; accepted January 5, 2025

This study focuses on the simulation and optimization of an InGaP/GaAs dual-junction solar cells using Silvaco Atlas software, with a special emphasis on the incorporation of a hetero tunnel junction. The hetero-tunnel junction plays a pivotal role in enabling efficient charge carrier transport between the sub-cells, significantly improving the overall cell efficiency. Additionally, a new back-surface field (BSF) layer was integrated into the GaAs bottom sub-cell to further enhance performance. Various material combinations for the hetero-tunnel junction such as GaInP/GaAs, AlGaInP/GaInP, and AlGaInP/GaAs were systematically tested to assess their influence on device efficiency. The optimized structure demonstrated a short-circuit current density of 1.780 mA/cm², an open-circuit voltage of 2.310 V, a fill factor of 86.501%, and a conversion efficiency of 35.57% under AM1.5G illumination at 300 K. Recombination losses were minimized by the BSF layer optimization in the top and bottom cell, particularly with AlGaInP, leading to improved charge collection. Elevated temperatures were found to reduce both the open-circuit voltage and efficiency, highlighting the necessity of thermal management. These optimizations represent significant improvements over prior designs.
Keywords: *InGaP/GaAs DJSCs; Solar cell; BSF; Silvaco-Atlas; Optimization*
PACS: 02.60.Cb, 02.60.Pn, 82.47.Jk, 84.60.Jt, 42.79.Ek, 89.30.Cc

INTRODUCTION

Solar cell technology remains one of the most effective methods for harnessing the sun's vast, renewable, and clean energy potential [1]**.** Photovoltaic conversion is the process by which electromagnetic energy is transformed directly into continuous electrical energy. This is achieved by converting photons from sunlight into electricity. This process is achieved through solar cells (photovoltaic cells) that incorporate optimized optoelectronic devices with reliable models. Solar radiation is the most abundant source of electromagnetic energy [2]. The solar photovoltaic research field is rapidly evolving, with continuous efforts aimed at reducing costs and enhancing efficiency. A notable approach to improving efficiency is spectrum splitting, which broadens the range of light absorbed across the solar spectrum [3]. Dual-junction solar cells (DJSCs), a leading innovation in photovoltaic (PV) technology, offer much higher conversion efficiencies than single-junction cells. This improvement is achieved through their two-layer structure, where each layer is optimized to absorb different parts of the solar spectrum. The top cell, with a higher bandgap, captures high-energy photons, while the bottom cell, with a lower bandgap, absorbs the lower-energy photons that pass through [4–6]. This complementary absorption of a wider range of sunlight boosts overall energy conversion efficiency. DJSCs, which incorporate this technique in a tandem structure, typically utilize III-V semiconductor materials like InGaP, GaAs, and Ge. These materials have different bandgaps, allowing for more efficient absorption across the solar spectrum [7].

In 2017, a study reported a 25.43% efficiency for an InGaP/GaAs hetero-junction solar cell by examining the influence of the window layer on performance at 300 K. The following year, another study achieved 34.44% efficiency by integrating a BSF and a TJ in an InGaP/GaAs structure [8]**.** The following year, another study achieved 34.44% efficiency by integrating a BSF and a TJ in an InGaP/GaAs structure [9]**.** Furthermore, Bin Zhao et al. introduced a thin layer into the structure of InGaP/GaAs DJSCs, improving the stability and performance of the cell's operational dynamics [10]. Tomah Sogabe et al. analyzed the impact of fluctuations in the intermediate band of InAs/GaAs solar cells, optimizing the efficiency and stability of these organometallic cells [11]. More recently, in 2023, optimization of an InGaP/GaAs DJSCs with dual tunnel junctions (TJs) and enhanced BSF layers resulted in an efficiency of 35.15% [12].

This paper aims to improve the efficiency of GaInP/GaAs DJSCs and identify the optimal output parameters of the structure. To achieve this, a DJSC comprising two sub-cells was simulated using Silvaco-Atlas software under standard AM1.5G illumination, with an incident power density of 100 mW/cm² and an ambient temperature of 300 K. First, numerical simulations were conducted to optimize the thickness of the new BSF layer in the bottom cell, aiming for favorable current matching between the upper and lower cells, which is essential for maximizing DJSC efficiency. Additionally, the material composition of the TJ was varied to explore potential improvements in conversion efficiency.

Cite as: I. Zidani, Z. Bensaad, L. Hafaifa, H. Abid, A. Hafaifa, East Eur. J. Phys. 1, 141 (2025), https://doi.org/10.26565/2312-4334-2025-1-13

Finally, the BSF layer in the upper cell was optimized, and the impact of temperature on the cell's performance parameters was investigated.

PARAMETERS FOR SIMULATION MODEL

Physical Models

The Physical modeling and simulation are critical for understanding device behavior and predicting performance, particularly in semiconductor devices like solar cells. Their main advantages cost-effectiveness, easy accessibility, and rapid implementation make them indispensable for optimizing and improving device designs. Among the available tools, Silvaco-Atlas is widely recognized as one of the most prominent simulation programs for solar cell modeling [13]. In this study, the physical models are divided into five core categories: mobility, recombination, carrier statistics, collision ionization, and tunneling. These models were carefully selected to match the material properties of the solar cell, ensuring accurate application throughout the device structure. Key parameters such as Shockley-Read-Hall (SRH) recombination and Band Gap Narrowing (BGN) are incorporated to capture critical mechanisms, including carrier recombination and the influence of heavy doping on the band structure. Operating temperature plays a significant role in device performance, primarily by affecting recombination dynamics. The SRH recombination model is particularly valued for its ability to replicate experimental results accurately, making it a standard approach in numerical simulations of solar cells. [8–10].

For the precise simulation of InGaP/GaAs DJSCs, especially in hetero tunnel junctions, specialized tunneling models are necessary. In this study, the BBT.NONLOCAL model is employed to account for non-local band-to-band tunneling, while the BBT model handles direct band-to-band transitions in regions with high electric fields. To ensure convergence during simulations, particularly when non-local coupling is present, the BBT.NLDERIVS model is recommended. The combination of these models enhances the accuracy and stability of the simulation results [11,12].

Key performance parameters critical to solar cell operation are derived from the *I-V* characteristics, represented by the *I-V* curve. The total current (*I*) in a solar cell consists of the sum of dark current and photocurrent (I_{ph}). This relationship is mathematically described by the Shockley equation [18]:

$$I = I_{ph} - I_0\left(\exp(\frac{qV}{akT}) - 1\right) \tag{1}$$

I is the net current flowing through the solar cell, V is the applied voltage, I_0 represents the saturation reverse current, a is the ideality factor, q denotes the electron charge, k is Boltzmann's constant, T is the absolute temperature.
The I_{SC} is defined as the current through the solar cell when V=0:

$$I_{sc} = I_{ph} \tag{2}$$

Key performance metrics, including the Jsc, Voc, and FF, can be calculated using the following equations:

$$V_{oc} = \frac{E_g}{q} - \frac{akT}{q}\ln(\frac{I_0}{I_{ph}}) \tag{3}$$

$$FF = \frac{P_{\max}}{V_{oc}J_{sc}} \tag{4}$$

Here P_{max} is the maximum power output of the solar cell.
The efficiency (η) of the solar cell is intrinsically linked to these parameters and is expressed as follows:

$$\eta = \frac{P_{max}}{P_{in}} = \frac{V_{oc}I_{sc}FF}{P_{in}} \tag{5}$$

Additionally, the recombination rates within the solar cell are modeled using the SRH mechanism, represented by the equation:

$$R_{n,p} = \frac{\sigma_n\sigma_p v_{th}N_t\left(np - n_i^2\right)}{\sigma_n\left[n + n_i\exp\left(\frac{E_t - E_i}{kT}\right)\right] + \sigma_p\left[p + n_i\exp\left(\frac{E_t - E_i}{kT}\right)\right]} \tag{6}$$

Where n_i is the intrinsic carrier density, v_{th} is the thermal velocity, σ_n and σ_p are the electron and hole capture cross sections, E_i and E_t represent the intrinsic Fermi energy level and trap energy level.

SIMULATED STRUCTURE

The structure of the simulated InGaP/GaAs DJSCs is illustrated in Figure 1, showcasing its intricate design aimed at optimizing both light absorption and charge carrier transport. This dual junction solar cell consists of a upper InGaP

cell and a lower GaAs cell, connected via a Hetero TJ (AlGaInP/GaAs). Each component is carefully engineered to maximize device performance.

The top InGaP cell features a p+/n+ junction, with a P+ InGaP emitter and an n+ InGaP base. With an energy Eg of 1.9 eV, this layer is optimized for capturing high-energy photons. To reduce surface recombination, a P+ AlInGaP window layer is positioned at the front of the top cell, enhancing overall efficiency. A BSF layer of n+ AlInGaP at the rear of the top cell further mitigates recombination by reflecting charge carriers.

The hetero tunnel junction that links the top and bottom cells is essential for seamless charge transport between them. This junction comprises an n+ AlInGaP layer and a p+ GaAs layer. These heavily doped layers facilitate efficient carrier tunneling with minimal resistance, ensuring strong electrical connectivity.

The bottom GaAs cell, with a p-n junction, has a lower energy Eg = 1.42 eV, targeting the absorption of lower-energy photons transmitted by the top cell. Its P+ GaAs emitter and n+ GaAs base are optimized for enhanced photon absorption. A P+ InGaP window layer further reduces surface recombination at the front, while two BSF layers (BSF1 and BSF2) of n+ AlInGaP ensure charge carrier reflection, minimizing recombination losses at the rear.

The entire cell architecture rests on an n+ GaAs substrate [19,20], which provides mechanical stability and enhanced electrical conductivity. A gold (Au) contact is employed at the cathode to facilitate efficient charge collection and conduction.

This meticulously engineered dual-junction configuration, leveraging the higher band-gap of InGaP and the lower band-gap of GaAs, enables efficient utilization of the solar spectrum. The design minimizes recombination losses and promotes effective charge transport, contributing to improved overall conversion efficiency. Additionally, the optical properties of the materials were sourced from the comprehensive SOPRA database available within the Silvaco-Atlas library [21]. All input parameters used in the simulations are presented in Table 1.

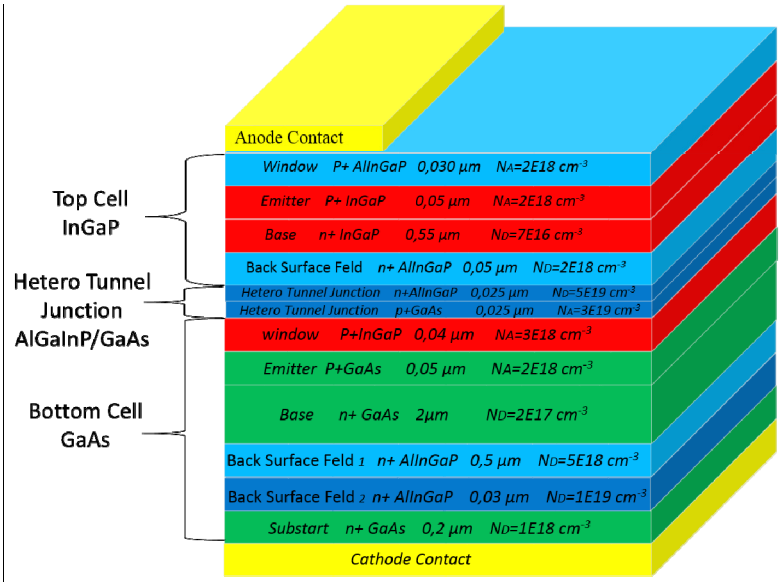

Figure 1. Schematic structure of InGaP/GaAs DJSCs.

Table 1. Summarizes the physical parameters of each material used in this simulation [22–24]**.**

Layer properties	AlGaInP	GaInP	GaAs	AlGaAs
Eg (eV)	2.3	1.9	1.42	1.8
α (Å)	5.56	5.56	5.56	5.64
es/eo	11.7	11.6	11.0	11.0
χ (eV)	4.2	4.16	4.07	4.1
Nc (cm^{-3})	1.2×10^{20}	1.30×10^{20}	4.7×10^{17}	4.35×10^{17}
Nv (cm^{-3})	1.28×10^{19}	1.28×10^{19}	7.0×10^{18}	8.16×10^{18}
MUN(cm^2/Vs)	2150	1945	8800	2000
MUP(cm^2/Vs)	141	141	400	138
τ_n(s)	1.00×10^{-9}	1.00×10^{-9}	1.00×10^{-9}	1.00×10^{-9}
τ_p (s)	1.00×10^{-9}	1.00×10^{-9}	2.00×0^{-8}	2.00×10^{-8}
n_i (per cc)	1	7.43×10^{4}	2.12×10^{6}	1

RESULTS AND DISCUSSION

The InGaP/GaAs DJSCs was simulated using the parameters outlined in Table 1, resulting in the J-V characteristics shown in Figure 2. This figure presents the I-V curves for the DJSCs, which features a GaAs/GaAs TJ. The individual I-V curves for the InGaP upper cell and GaAs lower cell are also depicted for comparison.

Under AM1.5G illumination, the design achieves a Jsc of 1.65×10^{-10}, Voc of 2.31 V, FF of 86.29%, and η of 32.83%. The tandem structure demonstrates efficient current matching between the sub-cells, with the I-V curves reflecting the performance of each junction within the stack.

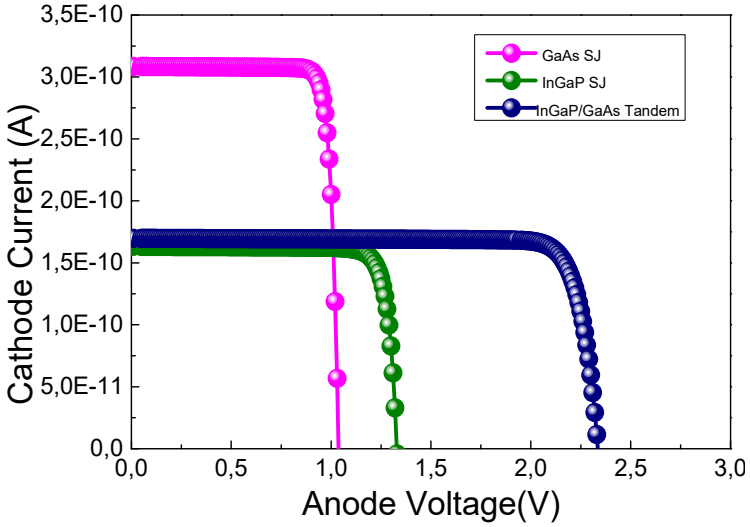

Figure 2. I-V Characteristics of InGaP/GaAs DJSCs

OPTIMIZATION OF THE NEW BSF LAYER IN THE GaAs BOTTOM CELL

The introduction of the quaternary compound AlInGaP as a BSF in the n-p GaAs bottom cell significantly influences the solar cell's performance metrics, as illustrated in Figure 3. The variation in BSF thickness from 0.01 µm to 0.04 µm reveals distinct trends across key parameters such as Jsc, Voc, FF, and η.

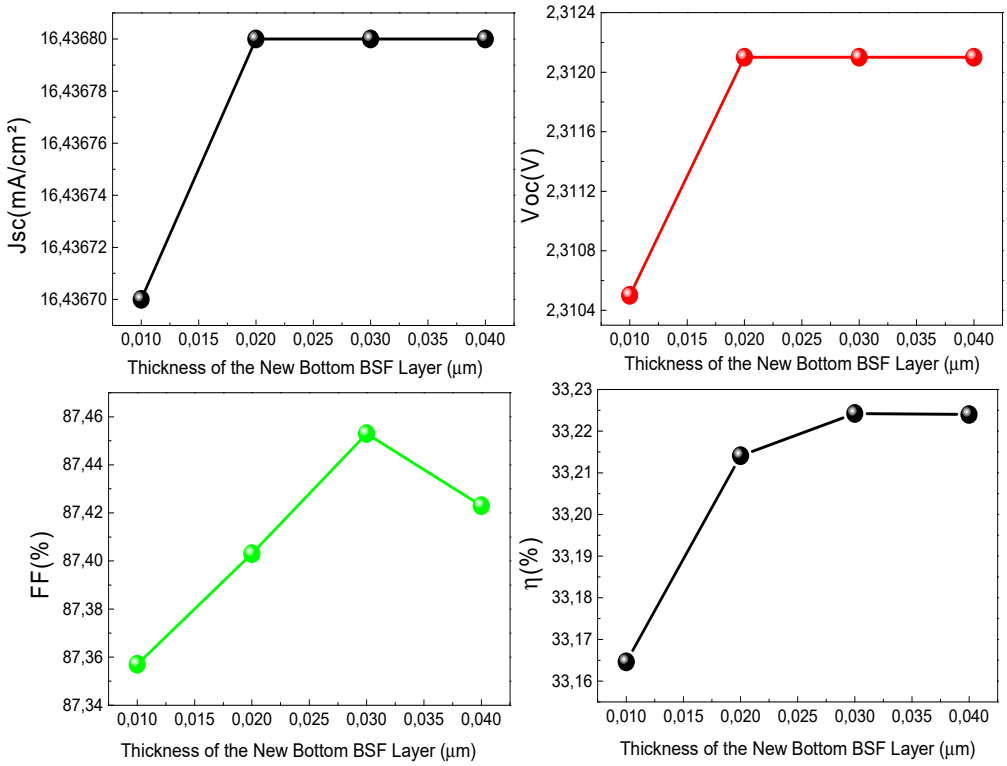

Figure 3. Impact of varying the thickness of the new bottom BSF layer on the η, FF, J_{SC}, and V_{OC} of the InGaP/GaAs DJSCs.

Jsc shows a sharp increase as the new bottom BSF thickness rises from 0.01 µm to 0.02 µm, reaching a stable maximum value of 16.436 mA/cm² beyond this point. Similarly, the Voc also increases with BSF thickness, stabilizing at 2.312 V for thicknesses greater than 0.02 µm.

The FF improves steadily as the new bottom BSF thickness increases from 0.01 µm, peaking at 87.46% at 0.03 µm. However, further increasing the new bottom BSF thickness results in a slight decline in FF, indicating that an overly thick BSF may hinder optimal carrier transport.

The overall efficiency follows a similar pattern, reaching its maximum value of 33.224% at a BSF thickness of 0.03 µm. Beyond this thickness, the efficiency begins to plateau, suggesting that 0.03 µm represents the optimal BSF thickness for this design. At this point, recombination losses are minimized, and photo-generated carrier transport is maximized, leading to the highest observed efficiency [7,12].

In conclusion, the optimal new bottom BSF thickness for this InGaP/GaAs DJSCs is identified at 0.03 µm, where the balance between reduced recombination losses and efficient carrier transport is achieved, as evidenced by the peak in both fill factor and overall efficiency. This highlights the critical role of BSF thickness in fine-tuning device performance for maximum output.

INFLUENCE OF HETERO-TJ MATERIALS ON InGaP/GaAs DJSCs PERFORMANCE

We further examined the impact of different hetero TJ materials by testing combinations of GaAs, AlGaAs, GaInP, and AlGaInP for the InGaP/GaAs DJSCs. The tunnel region facilitates the recombination of electrons and holes between the upper and lower cells, allowing current to flow in the DJSCs [20]. Figures 4 and 5 illustrate the I-V characteristics and conversion efficiency for various hetero TJ materials.

Among the combinations, the AlGaInP/GaAs hetero TJ exhibited the highest efficiency, reaching 34.31%, accompanied by a Jsc of 1.75 mA/cm² (as seen in Figure 5), a Voc of 2.36 V, and an FF of 87.19%. This makes AlGaInP/GaAs the optimal material combination in this study. The superior performance is attributed to the wider band-gap of AlGaInP, which reduces optical absorption compared to other materials, allowing lighter to reach the underlying layers. However, this higher band-gap increases the potential barrier, which slightly reduces the tunneling current in the diode.

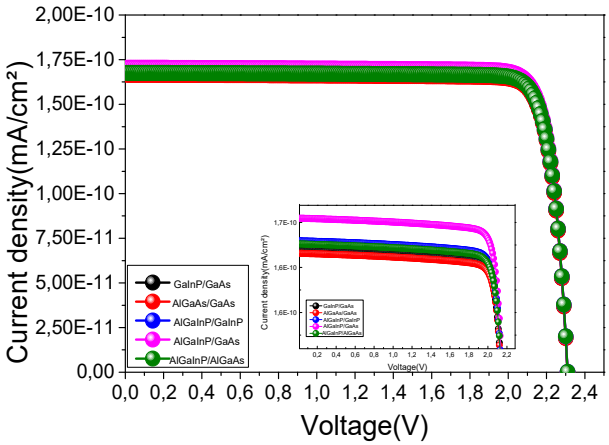

Figure 4. I-V Characteristics of InGaP/GaAs DJSCs with Different Tunnel Junctions

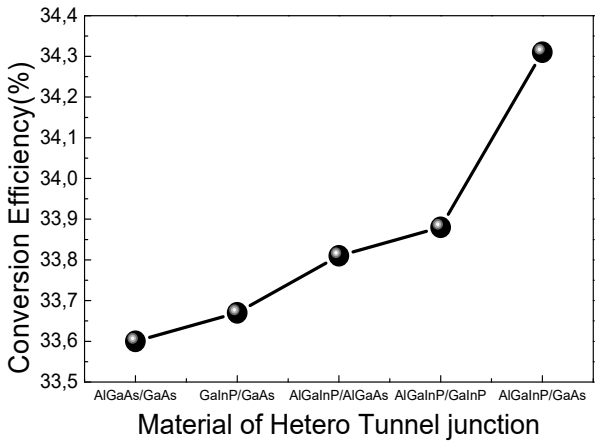

Figure 5. Impact of TJ Material on the Conversion Efficiency of InGaP/GaAs DJSCs

Similar trends were observed for AlGaAs/GaAs, GaInP/GaAs, AlGaInP/AlGaAs, and AlGaInP/GaInP combinations, though with comparatively lower efficiencies. Both the Jsc and η improved with the use of AlGaInP as the anode material in the hetero-tunnel junction, instead of GaAs. These results suggest that optimizing the hetero tunnel junction with AlGaInP can significantly enhance the efficiency of InGaP/GaAs DJSCs, primarily due to its favorable optical and electrical properties [25,26].

1.1. OPTIMIZATION OF BSF THICKNESS IN THE TOP SOLAR CELL

In this analysis, we systematically varied the thickness of the BSF layer in the upper cell while keeping all other parameters constant to assess its effect on the performance of the double-junction solar cell. As shown in Figure 6**,** the Jsc increases proportionally with efficiency as the thickness of the BSF layer grows. Notably, varying the BSF thickness from 0.01 to 0.05 µm has a significant impact on the overall efficiency of the cell.

The Jsc rises logarithmically from 16.61 to 17.805 mA/cm² as the thickness increases from 0.01 to 0.05 µm (Figure 6a). This indicates that the thicker BSF layer enhances carrier collection by minimizing recombination at the rear contact. Figure 6b shows that Voc **r**emains stable, holding at approximately 2.310 V across the range of BSF thicknesses. However, FF (Figure 6c) decreases slightly, reaching 86.5% at the thickest BSF layer. This reduction in FF is likely due to the increased series resistance associated with a thicker BSF layer, which can impede charge extraction.

Figure 6d illustrates that the overall η improves significantly as the BSF thickness increases. The efficiency rises from 33.53% to 35.57% as the thickness is varied from 0.01 to 0.05 µm, reflecting a logarithmic increase in performance. This enhancement can be attributed to better photo-generated carrier transport and reduced recombination, leading to higher current density and improved efficiency.

These findings underscore the importance of optimizing the BSF layer thickness to achieve higher efficiency in DJSCs, with the optimal thickness identified as 0.05 µm in this study. The results are consistent with those reported in previous studies [27,28], further validating the positive impact of a thicker BSF on cell performance.

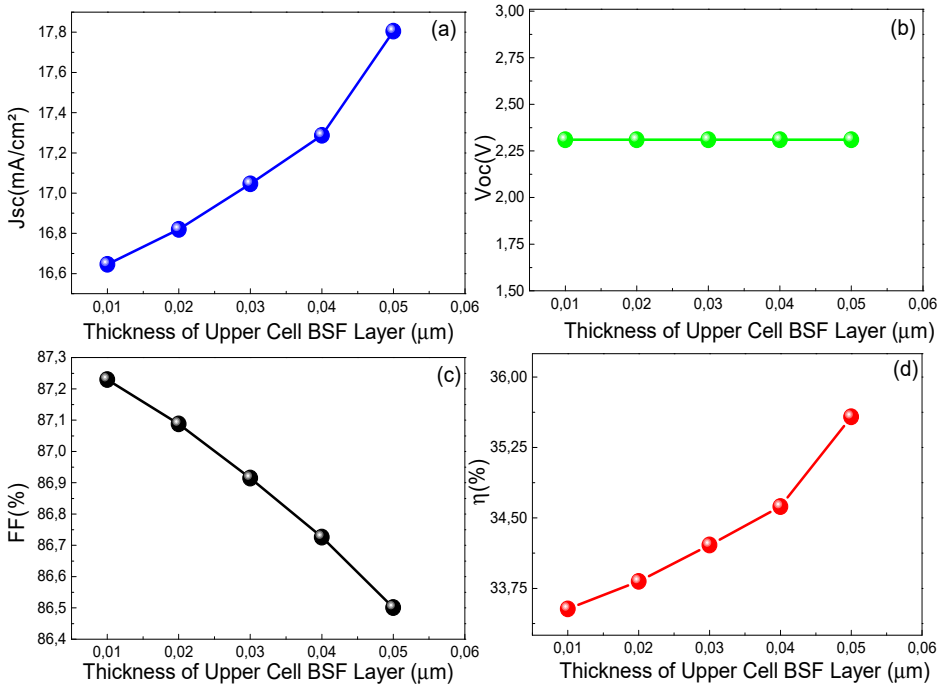

Figure 6. Effect of different BSF thickness of the upper cell on the η, FF, J_{SC}, and V_{OC} of the InGaP/GaAs DJSCs

Figure 7 illustrates the photo-generation rate for the proposed solar cell model, with values varying between 0 and 22.4 $cm^{-3}s^{-1}$. As seen in the figure, the highest photogeneration rates occur primarily in the upper layers of the solar cell, particularly in the InAlGaP and InGaP regions.

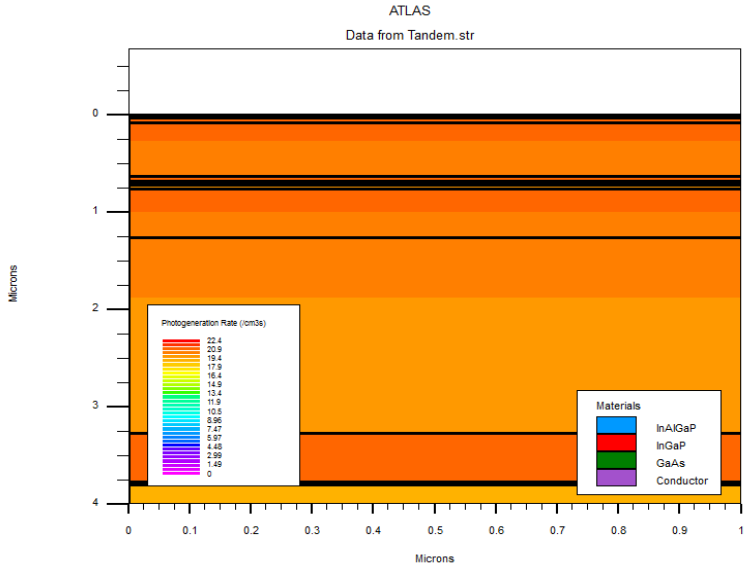

Figure 7. The photo-generation rate across various InGaP/GaAs DJSCs layers.

This is expected, as the majority of photon energy is absorbed near the surface before penetrating into the deeper layers of the device. The InAlGaP layer, in particular, demonstrates a superior photogeneration rate due to its higher absorption coefficient (α) compared to GaAs and InGaP. The increased absorption in this material allows for more efficient generation of electron-hole pairs, contributing significantly to the overall device performance. The highest photogeneration rates, exceeding 20 $cm^{-3}s^{-1}$, are concentrated in the InAlGaP layer, highlighting its critical role in enhancing the cell's optical and electrical performance.

Deeper into the cell, within the GaAs region, the photogeneration rate diminishes as most of the photon energy has already been absorbed in the upper layers. This trend underscores the importance of optimizing the thickness and material composition of the upper layers to maximize light absorption and improve the overall efficiency of the solar cell. These findings align with previous studies that emphasize the importance of material choice in achieving higher conversion efficiencies [20,29].

IMPACT OF TEMPERATURE FLUCTUATIONS

The temperature sensitivity of solar cells is a well-documented phenomenon, typical of semiconductor devices. As temperature increases, the band gap of the semiconductor decreases, which adversely affects the overall performance of the cell. This reduction in band gap is caused by the increased thermal energy within the material . As the temperature rises, less energy is required to break atomic bonds, thereby reducing the bond energy and, subsequently, the band gap. Consequently, higher temperatures result in a narrower energy gap in the solar cell. It is well-established that increasing the operating temperature of a solar cell leads to a reduction in both its efficiency and output power [30–32].

Figure 8(a) shows the variation in Jsc over a T range of 300 K to 400 K. While Jsc begins at 17.805 mA/cm² at 300 K, it gradually decreases to 17.760 mA/cm² at 400 K. This small reduction in Jsc indicates that it is relatively stable over this temperature range, suggesting that the InGaP/GaAs tandem cell's Jsc is less sensitive to temperature compared to other parameters.

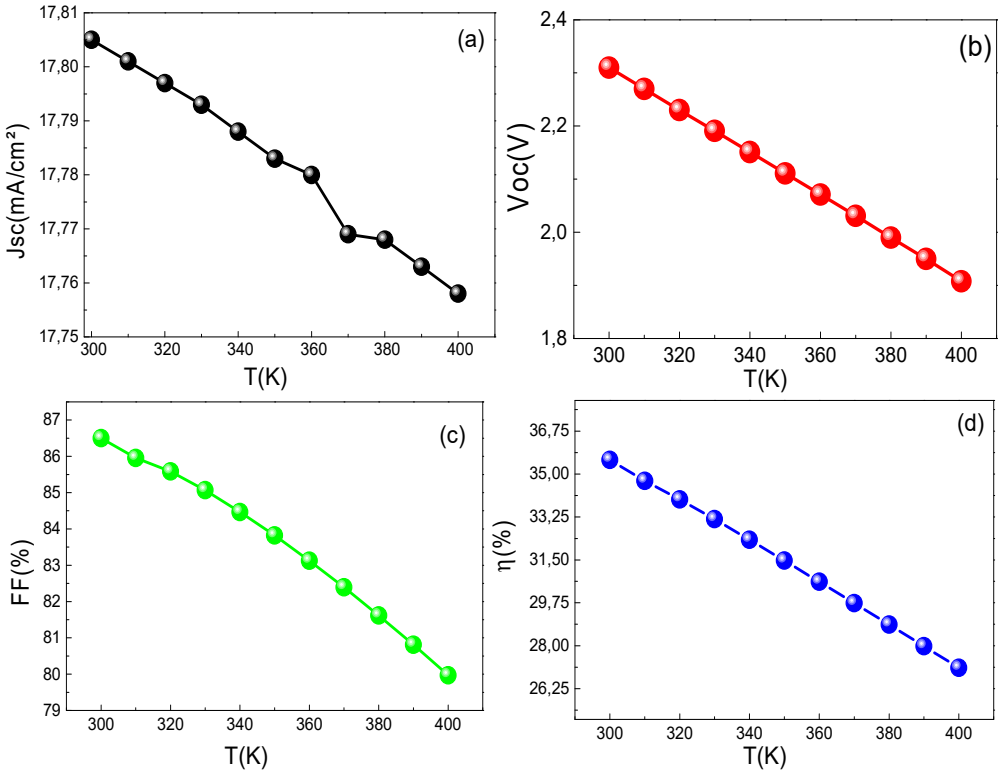

Figure 8. Impact of temperature on the InGaP/GaAs DJSCs performance.

Figure 8(b) highlights the significant impact of temperature on Voc. As the temperature increases from 300 K to 400 K, Voc steadily declines from 2.310 V to 1.908 V, indicating a strong temperature sensitivity. This reduction in Voc, governed by Eq. (3), is the primary factor behind the overall decline in performance parameters. The efficiency decreases markedly at higher temperatures due to this drop in Voc, which can be attributed to the temperature-induced narrowing of the band gap. As the band gap shrinks, the maximum achievable voltage of the cell is reduced, directly affecting its performance.

The FF, as shown in Figure 8(c), also decreases as the temperature increases. FF declines from 86.501% at 300 K to 79.970% at 400 K. This decline reflects a reduced ability of the solar cell to deliver its maximum power as the temperature rises, likely due to increased recombination losses [32,33].

Most critically, Figure 8(d) shows a linear decrease in the η of the solar cell. Efficiency falls from 35.57% at 300 K to 26.253% at 400 K. This significant reduction in efficiency, more than 10 percentage points, highlights the detrimental effect of elevated temperatures on the performance of the solar cell. The efficiency decline is primarily due to increased recombination losses, and reduced Voc at higher temperatures.

In summary, the data presented clearly demonstrate the negative impact of rising temperature on the performance of the InGaP/GaAs DJSCs. As temperature increases from 300 K to 400 K, all key performance metrics Jsc, Voc, FF, and η Experience declines. Notably, the efficiency of the cell peaks at 35.57% at 300 K, corresponding to optimal performance at lower temperatures. This highlights the importance of temperature management in maintaining the efficiency and longevity of solar cells in practical applications.

OPTIMIZED InGaP/GaAs DJSCs

The output parameters of the optimized InGaP/GaAs DJSCs are presented in **Table 2**, offering a comparative analysis of experimental and theoretical values from various studies. Notably, the tandem cell developed in this work

demonstrates strong performance across key metrics, positioning it competitively within the field. The Jsc of the DJSCs in this study is 1.7805 mA/cm², which exceeds both the theoretical values reported in [8,9], and [12], as well as the experimental value of 1.61 mA/cm² from [20]. This higher Jsc indicates an improvement in current collection, likely due to the optimization of the tandem structure, which enhances light absorption and carrier generation.

The η of the tandem cell, at 35.57%, represents a significant improvement over both the experimental result of 32.19% from [20] and the theoretical values from [8,9]. This substantial increase in efficiency highlights the effectiveness of the optimized hetero-tunnel junction design (n-AlInGaP/p-GaAs) used in this work, which minimizes recombination losses and maximizes power output.

Table. 2 Comparative analysis of performance parameters for optimized InGaP/GaAs DJSC structure compared to other designs.

	Jsc (mA/cm^2)	Voc (V)	FF (%)	η (%)
InGaP/GaAs DJSCs (Theoretical) [8]	1.519	2.53	91.32	25.43
InGaP/GaAs DJSCs (Experimental)[20]	1.61	2.39	87.52	32.19
InGaP/GaAs DJSCs (Theoretical) [9]	1.449	2.62	90.68	34.44
InGaP/GaAs DJSCs (Theoretical) [12]	1.613	2.45	88.80	35.15%
Our Simulation	1.780	2.310	86.501	35.57

The I-V characteristics for the GaInP/GaAs DJSCs, displayed in Figure 9**,** compare the performance of the fundamental design with the improved version. The improved cell shows a clear enhancement in both current and voltage stability across the operating range. This improved performance suggests more efficient charge carrier collection and superior voltage retention, leading to higher overall power output.

In conclusion, the optimization strategies applied in this work, particularly the design of the hetero-tunnel junction, have resulted in a significant boost in both Jsc and η, demonstrating that this tandem solar cell outperforms previous designs and represents a notable advancement in the field of high-efficiency DJSCs.

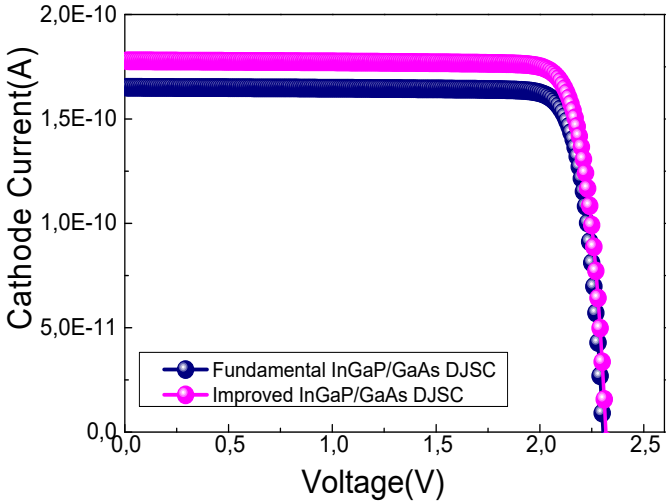

Figure 9. I-V Characteristic of InGaP/GaAs DJSCs.

CONCLUSIONS

This study utilized advanced numerical simulations via Silvaco Atlas to assess and optimize the performance of an InGaP/GaAs dual-junction solar cells. A new BSF layer was incorporated into the bottom cell, and various hetero-tunnel junction materials were systematically evaluated. The results indicated that the optimal performance was achieved with a new bottom BSF layer of 0.03 μm, composed of InAlGaP, resulting in an efficiency of 33.224%. Among the hetero-tunnel junction materials tested, the InAlGaP/GaAs combination demonstrated superior efficiency and overall performance enhancements. Furthermore, optimizing a BSF layer with a thickness of 0.05 μm to the upper cell significantly increased the overall efficiency to 35.57%. The optimized dual-junction structure achieved Jsc of 1.780 mA/cm², Voc of 2.310 V, FF of 86.501%, and η of 35.57% at 300 K. These results highlight the effectiveness of simulation-driven approaches in optimizing multi-junction solar cell designs, offering a cost-effective method to reduce prototyping efforts by focusing experimental validation on a refined set of high-performance configurations.

Acknowledgement

The authors are thankful to the DGRSDT for the provided support to accomplish this research.

ORCID

Ikram Zidani, https://orcid.org/0009-0003-8900-5261; **Loumafak Hafaifa,** https://orcid.org/0009-0000-0900-759X
Ahmed Hafaifa, https://orcid.org/0000-0002-7812-7429

REFERENCES

[1] N. Akter, M.A. Matin, and N. Amin, "High performance $In_xGa_{1-x}N$ Tandem solar cells designed from numerical analysis," in: *CEAT 2013 - 2013 IEEE Conf. Clean Energy Technol*, 2013, pp. 469–472. https://doi.org/10.1109/CEAT.2013.6775678
[2] J.B. Garcia, *Indium Gallium Nitride Multijunction Solar Cell Simulation Using Silvaco Atlas*, Security, 110, (2007)
[3] C. Cornet, M. Da Silva, C. Levallois, and O. Durand, "GaP/Si-based photovoltaic devices grown by molecular beam epitaxy," in: *Molecular Beam Epitaxy*, second edition), (2018), pp. 637–648. https://doi.org/10.1016/B978-0-12-812136-8.00030-X
[4] L. Hafaifa, M. Maache, and M.W. Bouabdelli, "Improving the Performance of CZTS/CZTSSe Tandem Thin Film Solar Cell," J. Nano- Electron. Phys. **16**, 1–6 (2024). https://doi.org/10.21272/jnep.16(2).02018
[5] E. Raza, and Z. Ahmad, "Review on two-terminal and four-terminal crystalline-silicon/perovskite tandem solar cells; progress, challenges, and future perspectives," Energy Reports, **8**, 5820–5851 (2022). https://doi.org/10.1016/j.egyr.2022.04.028
[6] L. Hafaifa, M. Maache, and Y. Djalab, "Performance Enhancement of CGS/CIGS Thin Flm Tandem Solar Cell Using Different Buffer Layers," J. Opt. (2024). https://doi.org/10.1007/s12596-024-02035-1
[7] A. Ghadimi, and H. Arzbin, "Efficiency improvement of ARC less InGaP/GaAs DJ solar cell with InGaP tunnel junction and optimized two BSF layer in top and bottom cells," Optik, **148**, 358–367 (2017). https://doi.org/10.1016/j.ijleo.2017.09.016
[8] F. Djaafar, B. Hadri, and G. Bachir, "Optimal parameters for performant heterojunction InGaP/GaAs solar cell," Int. J. Hydrogen Energy, **42**, 8644–8649 (2017). https://doi.org/10.1016/j.ijhydene.2016.06.139
[9] F. Djaafar, B. Hadri, and G. Bachir, "IV Characteristics of InGaP/GaAs Solar Cell with the presence of a Back Surface Field and a Tunnel junction," J. Electr. Syst. **14**, 64–76 (2018).
[10] B. Zhao, X.-S. Tang, W.-X. Huo, Y. Jiang, Z.-G. Ma, L. Wang, W.-X. Wang, *et al*., "Characteristics of InGaP/GaAs double junction thin film solar cells on a flexible metallic substrate," Sol. Energy, **174**, 703–708 (2018). https://doi.org/10.1016/j.solener.2018.06.099
[11] T. Sogabe, Y. Shoji, N. Miyashita, D.J. Farrell, K. Shiba, H.-F. Hong, and Y. Okada, "High-efficiency InAs/GaAs quantum dot intermediate band solar cell achieved through current constraint engineering," Next Mater. **1**, 100013 (2023). https://doi.org/10.1016/j.nxmate.2023.100013
[12] F.Z. Kharchich, and A. Khamlichi, "Optimizing efficiency of InGaP/GaAs dual-junction solar cells with double tunnel junction and bottom back surface field layers," Optik, **272**, 170196 (2023). https://doi.org/10.1016/j.ijleo.2022.170196
[13] L. Hafaifa, M. Maache, Z. Allam, and A. Zebeir, "Simulation and performance analysis of CdTe thin film solar cell using different Cd-free zinc chalcogenide-based buffer layers," Results Opt. **14**, 100596 (2024). https://doi.org/10.1016/j.rio.2023.100596
[14] J.L. Gray, *Handbook of Photovoltaic Science and Engineering*, Chapter 3, (John Wiley & Sons, Ltd, 2003), pp. 61–112.
[15] M.H. Tsutagawa, and S. Michael, "Triple junction InGaP/GaAS/Ge solar cell optimization: the design parameters for a 36.2% efficient space cell using Silvaco ATLAS modeling & simulation," in: *2009 34th IEEE Photovolt. Spec. Conf. IEEE*, (2009), pp. 1954–1957. https://doi.org/10.1109/PVSC.2009.5411544
[16] J.E. VanDyke, "Modeling laser effects on multi-junction solar cells using Silvaco ATLAS software for spacecraft power beaming applications, PhD Thesis. Monterey, California. Naval Postgraduate School, 2010.
[17] J.B. Lavery, "Quantum tunneling model of a pn junction in Silvaco," PhD Thesis. Monterey, California. Naval Postgraduate School, (2008).
[18] L. Hafaifa, M. Maache, and M.W. Bouabdelli, "Improved performance of CdTe thin-film solar cell through key parameters," J. Theor. Appl. Phys. **18**, 1–10 (2024). https://doi.org/10.57647/j.jtap.2024.1803.35
[19] R.R. King, N.H. Karam, J.H. Ermer, N. Haddad, P. Colter, T. Isshiki, H. Yoon, *et al*., "Next-generation, high-efficiency III-V multijunction solar cells," in: *Conf. Rec. Twenty-Eighth IEEE Photovolt. Spec. Conf. (Cat. No. 00CH37036), IEEE*, 2000, pp. 998–1001. https://doi.org/10.1109/PVSC.2000.916054
[20] K.J. Singh, and S.K. Sarkar, "Highly efficient ARC less InGaP/GaAs DJ solar cell numerical modeling using optimized InAlGaP BSF layers," Opt. Quantum Electron. **43**, 1–21 (2012). https://doi.org/10.1007/s11082-011-9499-y
[21] Atlas User's Manual, SILVACO Inc, Santa Clara, CA 95054, California, USA, 2018.
[22] I. Vurgaftman, J.A.R. Meyer, and L.R. Ram-Mohan, "Band parameters for III–V compound semiconductors and their alloys," J. Appl. Phys. **89**, 5815–5875 (2001). https://doi.org/10.1063/1.1368156
[23] S. Abbasian, and R. Sabbaghi-Nadooshan, "Design and evaluation of ARC less InGaP/AlGaInP DJ solar cell," Optik, **136**, 487–496 (2017). https://doi.org/10.1016/j.ijleo.2017.02.078
[24] G.S. Sahoo, and G.P. Mishra, "Effective use of spectrum by an ARC less dual junction solar cell to achieve higher efficiency: a simulation study," Superlattices Microstruct. **109**, 794–804 v. https://doi.org/10.1016/j.spmi.2017.06.002
[25] G.S. Sahoo, P.P. Nayak, and G.P. Mishra, "An ARC less InGaP/GaAs DJ solar cell with hetero tunnel junction," Superlattices Microstruct. **95**, 115–127 (2016). https://doi.org/10.1016/j.spmi.2016.04.045
[26] S.M. Sze, Y. Li, and K.K. Ng, *Physics of semiconductor devices*, (John wiley & sons, 2021).
[27] M. Verma, and G.P. Mishra, "An integrated GaInP/Si dual-junction solar cell with enhanced efficiency using TOPCon technology," Appl. Phys. A Mater. Sci. Process. **126**, 1–13 (2020). https://doi.org/10.1007/s00339-020-03840-8
[28] S. Bagheri, R. Talebzadeh, B. Sardari, and F. Mehdizadeh, "Design and simulation of a high efficiency InGaP/GaAs multi junction solar cell with AlGaAs tunnel junction," Optik, **199**, 163315 (2019). https://doi.org/10.1016/j.ijleo.2019.163315
[29] H.R. Arzbin, and A. Ghadimi, "Improving the performance of a multi-junction solar cell by optimizing BSF, base and emitter layers," Mater. Sci. Eng. B, **243**, 108–114 (2019). https://doi.org/10.1016/j.mseb.2019.04.001
[30] Y.P. Varshni, "Temperature dependence of the energy gap in semiconductors," Physica, **34**, 149–154 (1967). https://doi.org/10.1016/0031-8914(67)90062-6
[31] H.M. Ali, M. Mahmood, M.A. Bashir, M. Ali, and A.M. Siddiqui, "Outdoor testing of photovoltaic modules during summer in Taxila, Pakistan," Therm. Sci. **20**, 165–173 (2016). https://doi.org/10.2298/TSCI131216025A
[32] L. Hafaifa, M. Maache, S. Rabhi, Z. Allam, Z.I. Gouchida, Y. Benbouzid, A. Zebeir, and R. Adjouz, "Enhanced CZTSSe Thin-Film Solar Cell Efficiency: Key Parameter Analysis," Phys. Status Solidi Appl. Mater. Sci. **222**(2), 2400332 1–8 (2024). https://doi.org/10.1002/pssa.202400332

[33] E.T. Mohamed, A.O.M. Maka, M. Mehmood, Al.M. Direedar, and N. Amin, "Performance simulation of single and dual-junction GaInP/GaAs tandem solar cells using AMPS-1D," Sustain. Energy Technol. Assessments, **44**, 101067 (2021). https://doi.org/10.1016/j.seta.2021.101067

ПІДВИЩЕННЯ ПРОДУКТИВНОСТІ СОНЯЧНИХ ЕЛЕМЕНТІВ З ПОДВІЙНИМ ПЕРЕХОДОМ InGaP/GaAs ЧЕРЕЗ ОПТИМІЗАЦІЮ ШАРУ BSF ТА ГЕТЕРОТУНЕЛЬНИЙ ПЕРЕХІД

Ікрам Зідані[a], Зуауї Бенсаад[a], Лумафак Хафайфа[b,c], Хамза Абід[a], Ахмед Хафайфа[d]

[a]Лабораторія прикладних матеріалів, Університет Джілалі Ліабес, Сіді-Бель-Аббес, Алжир

[b]Кафедра фізики, факультет точних наук і комп'ютерних наук, Університет Зіана Ашура, 17000 Джельфа, Алжир

[c]Лабораторія фізико-хімії матеріалів та навколишнього середовища, Університет Зіан Ашур, BP 3117, Джельфа, Алжир

[d]Лабораторія прикладної автоматизації та промислової діагностики, факультет науки і технологій, Університет Джельфи 17000 DZ, Алжир

Це дослідження зосереджено на моделюванні та оптимізації подвійних сонячних елементів InGaP/GaAs з використанням програмного забезпечення Silvaco Atlas, з особливим акцентом на впровадженні гетеротунельного переходу. Гетеротунельний перехід відіграє ключову роль у забезпеченні ефективного транспортування носіїв заряду між субелементами, значно покращуючи загальну ефективність клітини. Крім того, новий шар поля зворотної поверхні (BSF) був інтегрований у нижню частину GaAs для подальшого підвищення продуктивності. Різні комбінації матеріалів для гетеротунельного переходу, такі як GaInP/GaAs, AlGaInP/GaInP і AlGaInP/GaAs, систематично перевірялися, щоб оцінити їх вплив на ефективність пристрою. Оптимізована структура продемонструвала щільність струму короткого замикання 1,780 мА/см², напругу холостого ходу 2,310 В, коефіцієнт заповнення 86,501% і ефективність перетворення 35,57% під освітленням AM1.5G при 300 K. Втрати на рекомбінацію були мінімізовані оптимізацією шару BSF у верхній і нижній комірках, зокрема з AlGaInP, що сприяє покращенню збору заряду. Виявлено, що підвищені температури знижують як напругу холостого ходу, так і ефективність, що підкреслює необхідність керування температурою. Ці оптимізації представляють значні покращення порівняно з попередніми проектами.

Ключові слова: *InGaP/GaAs DJSCs; сонячна батарея; BSF, Silvaco-Atlas; оптимізація*